Zero background fluorescent probe for sensing and imaging of glutathione via the "covalent-assembly" approach

Zheng Yang,* Zhiyao Wang, Ying Peng, Hao Yang, Qian Wang, Xiaodan Jia, and Xiangrong Liu

College of Chemistry and Chemical Engineering, Xi'an University of Science and Technology, Xi'an 710054, P. R. China.

*Corresponding author: yangzheng@xust.edu.cn; orcid.org/0000-0002-1554-4794.

CONTENTS

1. Optical properties of the probe.

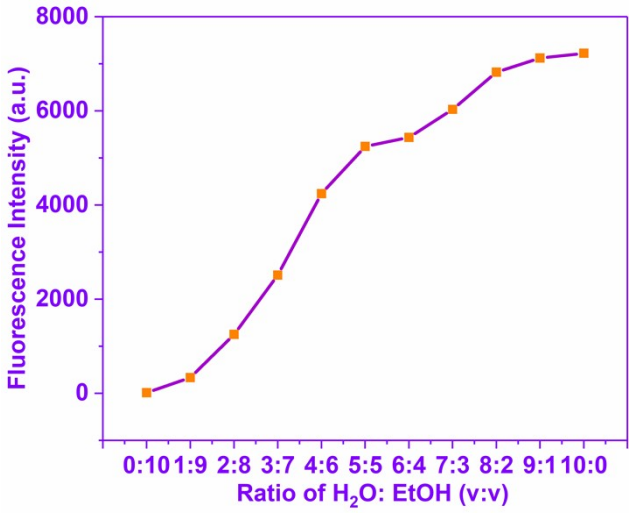

Fig. S1 Fluorescence intensity of probe ***R1*** (20 μmol·L^{-1}) in presence of 25 equiv. of GSH in different EtOH-H_2O solutions with PBS buffer (0.1 mol·L^{-1}, pH 7.4), λ_{ex} = 430 nm.

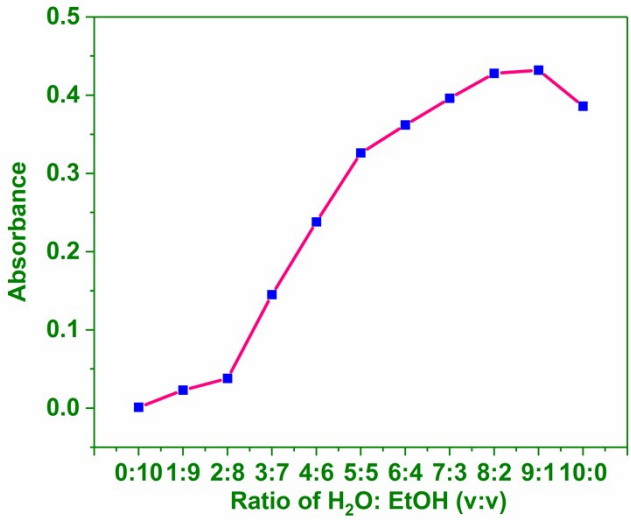

Fig. S2 Absorbance of probe ***R1*** (20 μmol·L^{-1}) in presence of 25 equiv. of GSH in different EtOH-H_2O solutions with PBS buffer (0.1 mol·L^{-1}, pH 7.4).

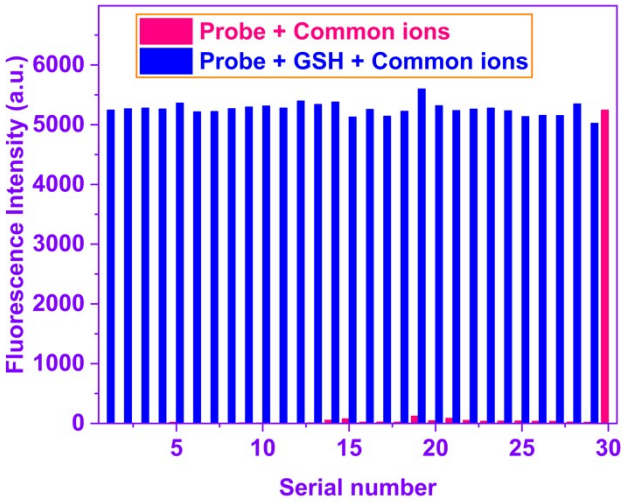

Fig. S3 Fluorescence intensity changes of probe ***R1*** (20 μmol·L^{-1}) in EtOH-H_2O (1:1, v/v, PBS, pH 7.4) over the analytes of interest (500 μmol·L^{-1}). Pink bars represent the fluorescence response of probe ***R1*** to: 1, blank, 2, Na^+, 3, K^+, 4, Ag^+, 5, Ca^{2+}, 6, Mg^{2+}, 7, Cu^{2+}, 8, Cd^{2+}, 9, Mn^{2+}, 10, Fe^{2+}, 11, Co^{2+}, 12, Ni^{2+}, 13, Zn^{2+}, 14, Pb^{2+}, 15, Hg^{2+}, 16, Fe^{3+}, 17, Cr^{3+}, 18, Al^{3+}, 19, Sn^{4+}, 20, $O_2^{\cdot-}$, 21, H_2O_2, 22, NO, 23, $ONOO^-$, 24, NO_3^-, 25, PO_4^{3-}, 26, CO_3^{2-}, 27, OAc^-, 28, $C_2O_4^{2-}$, 29, ClO^-, 30, GSH. Blue bars represent the fluorescence response with subsequent addition of 25 equiv. of GSH to the above solutions, λ_{ex} = 430 nm.

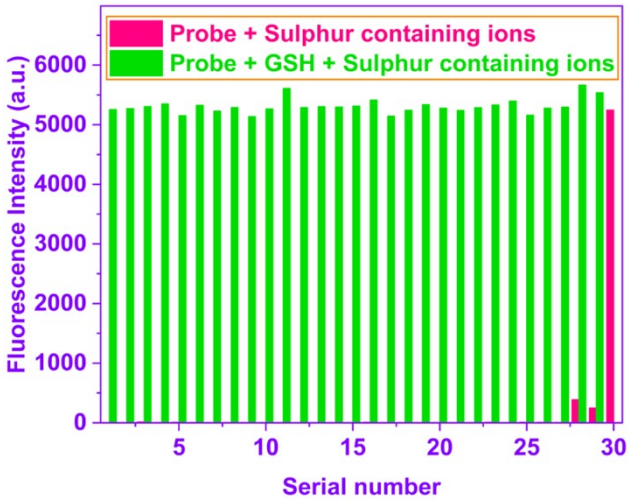

Fig. S4 Absorbance changes of probe ***R1*** (20 μmol·L^{-1}) in EtOH-H_2O (5:5, v/v, PBS, pH 7.4) over the analytes of interest (500 μmol·L^{-1}). Green bars represent the fluorescence response of probe ***R1*** to: 1, blank, 2, Na^+, 3, K^+, 4, Ag^+, 5, Ca^{2+}, 6, Mg^{2+}, 7, Cu^{2+}, 8, Cd^{2+}, 9, Mn^{2+}, 10, Fe^{2+}, 11, Co^{2+}, 12, Ni^{2+}, 13, Zn^{2+}, 14, Pb^{2+}, 15, Hg^{2+}, 16, Fe^{3+}, 17, Cr^{3+}, 18, Al^{3+}, 19, Sn^{4+}, 20, $O_2^{\cdot-}$, 21, H_2O_2, 22, NO, 23, $ONOO^-$, 24, NO_3^-, 25, PO_4^{3-}, 26, CO_3^{2-}, 27, OAc^-, 28, $C_2O_4^{2-}$, 29, ClO^-, 30, GSH. Pink bars represent the fluorescence response with subsequent addition of 25 equiv. of GSH to the above solutions.

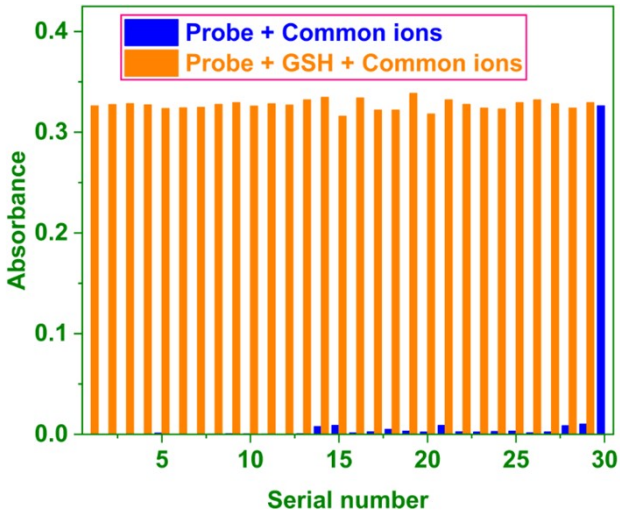

Fig. S5 Fluorescence intensity changes of probe ***R1*** (20 μmol·L^{-1}) in EtOH-H_2O (5:5, v/v, PBS, pH 7.4) over the analytes of interest (500 μmol·L^{-1}). Blue bars represent the fluorescence response of probe ***R1*** to: 1. Ala, 2. Arg, 3. Glu, 4. Ile, 5. Leu, 6. Lys, 7. Met, 8. Phe, 9. Pro, 10. Ser, 11. Thr, 12. Trp, 13. Tyr, 14. Val, 15. Sec, 16. AA, 17. H_2S, 18. HS^-, 19. SO_3^{2-}, 20. HSO_3^-, 21. $S_2O_3^{2-}$, 22. SO_4^{2-}, 23. HSO_4^-, 24. S_8, 25. Na_2S_2, 26. Na_2S_4, 27. PhSH, 28. Cys, 29. Hcy, 30. GSH. Orange bars represent the fluorescence response with subsequent addition of 25 equiv. of GSH to the above solutions, λ_{ex} = 430 nm.

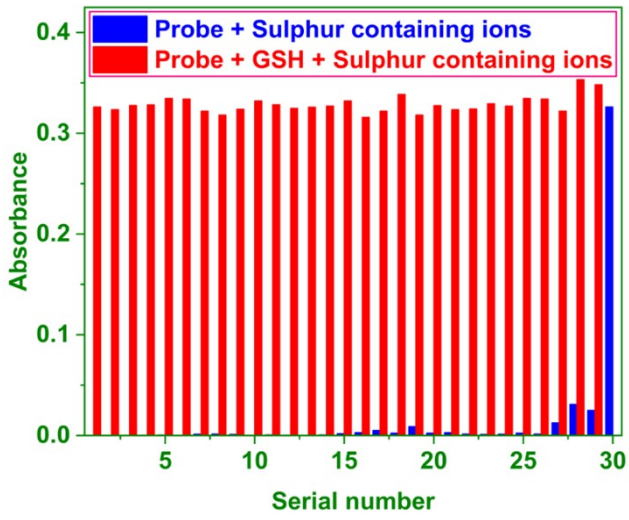

Fig. S6 Absorbance changes of probe ***R1*** (20 μmol·L^{-1}) in EtOH-H_2O (5:5, v/v, PBS, pH 7.4) over the analytes of interest (500 μmol·L^{-1}). Blue bars represent the fluorescence response of probe ***R1*** to: 1. Ala, 2. Arg, 3. Glu, 4. Ile, 5. Leu, 6. Lys, 7. Met, 8. Phe, 9. Pro, 10. Ser, 11. Thr, 12. Trp, 13. Tyr, 14. Val, 15. Sec, 16. AA, 17. H_2S, 18. HS^-, 19. SO_3^{2-}, 20. HSO_3^-, 21. $S_2O_3^{2-}$, 22. SO_4^{2-}, 23. HSO_4^-, 24. S_8, 25. Na_2S_2, 26. Na_2S_4, 27. PhSH, 28. Cys, 29. Hcy, 30. GSH. Red bars represent the fluorescence response with subsequent addition of 25 equiv. of GSH to the above solutions.

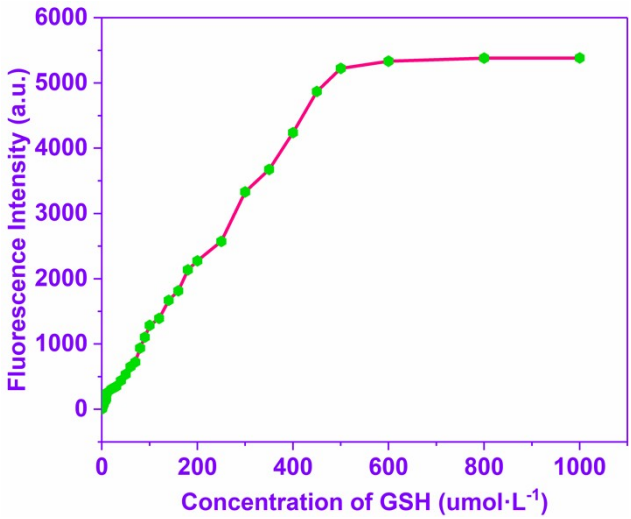

Fig. S7 Fluorescence intensity change of probe ***R1*** (20 μmol·L^{-1}) in EtOH-H_2O (1:1, v/v, PBS, pH 7.4) solution as a function of thiols concentration at 540 nm, λ_{ex} = 430 nm.

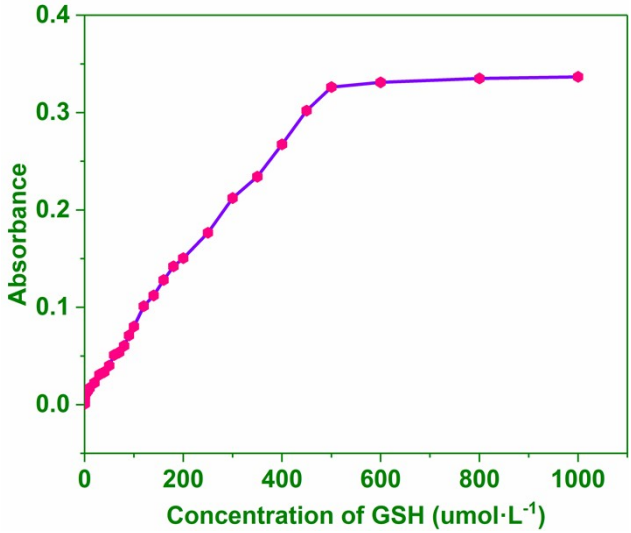

Fig. S8 Absorption intensity change of probe ***R1*** (20 μmol·L^{-1}) in EtOH-H_2O (1:1, v/v, PBS, pH 7.4) solution as a function of thiols concentration at 509 nm.

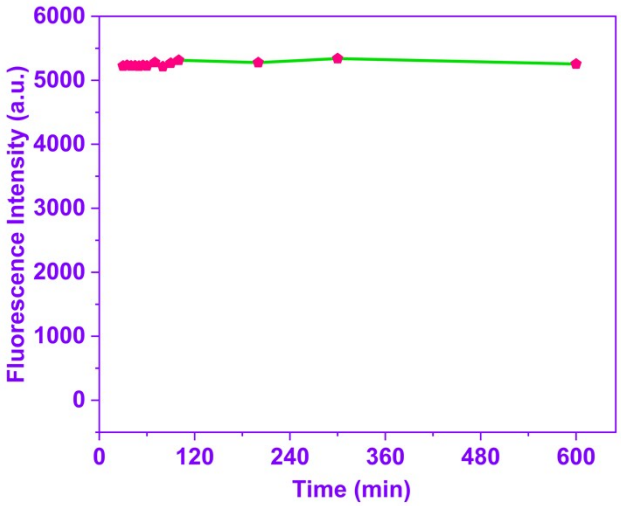

Fig. S9 Fluorescence intensity change of probe ***R1*** (20 μmol·L^{-1}) upon addition of GSH (500 μmol·L^{-1}) with different reaction time in EtOH–H_2O (1:1, v:v, PBS, pH = 7.4) solution., λ_{ex} = 430 nm.

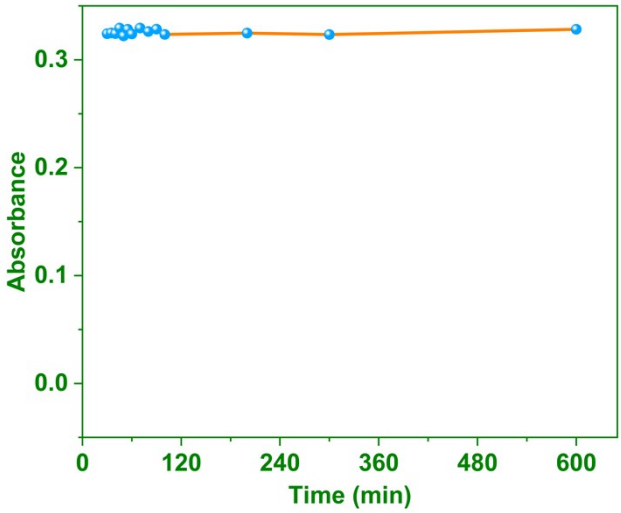

Fig. S10 Absorption intensity change of probe ***R1*** (20 μmol·L^{-1}) upon addition of GSH (500 μmol·L^{-1}) with different reaction time in EtOH–H_2O (1:1, v:v, PBS, pH = 7.4) solution.

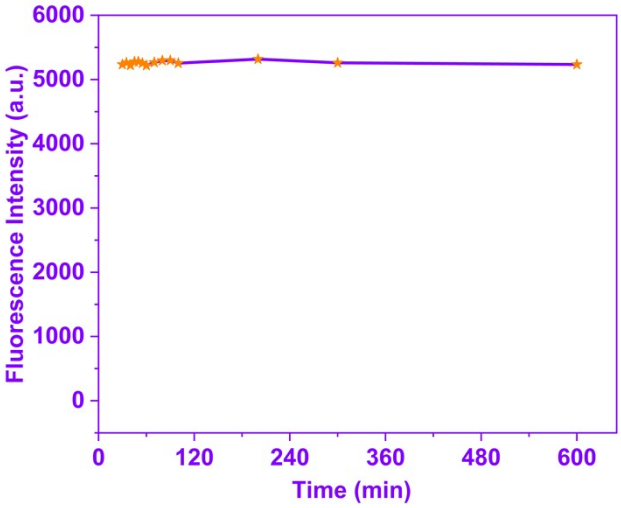

Fig. S11 Fluorescence intensity change of probe ***R1*** (20 μmol·L^{-1}) upon addition of GSH (500 μmol·L^{-1}) under the presence of contentious irradiation by 254 nm UV in EtOH–H_2O (1:1, v:v, PBS, pH = 7.4) solution, λ_{ex} = 430 nm.

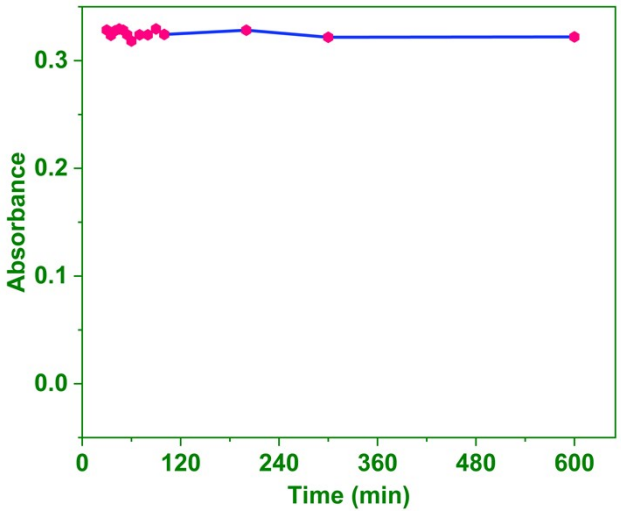

Fig. S12 Absorption intensity change of probe ***R1*** (20 μmol·L^{-1}) upon addition of GSH (500 μmol·L^{-1}) under the presence of contentious irradiation by 254 nm UV in EtOH–H_2O (1:1, v:v, PBS, pH = 7.4) solution.

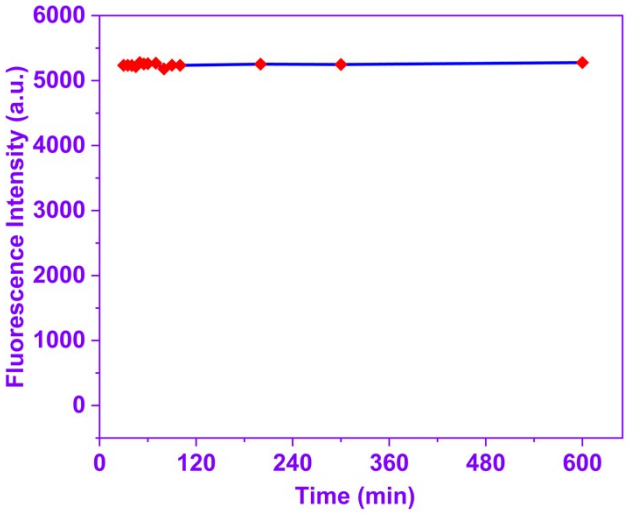

Fig. S13 Fluorescence intensity change of probe ***R1*** (20 μmol·L^{-1}) upon addition of GSH (500 μmol·L^{-1}) under the presence of contentious irradiation by 365 nm UV in EtOH–H_2O (1:1, v:v, PBS, pH = 7.4) solution, λ_{ex} = 430 nm.

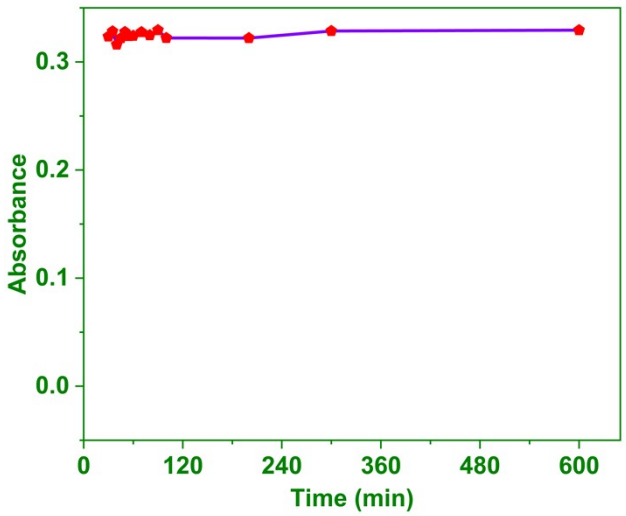

Fig. S14 Absorption intensity change of probe ***R1*** (20 μmol·L^{-1}) upon addition of GSH (500 μmol·L^{-1}) under the presence of contentious irradiation by 365 nm UV in EtOH–H_2O (1:1, v:v, PBS, pH = 7.4) solution.

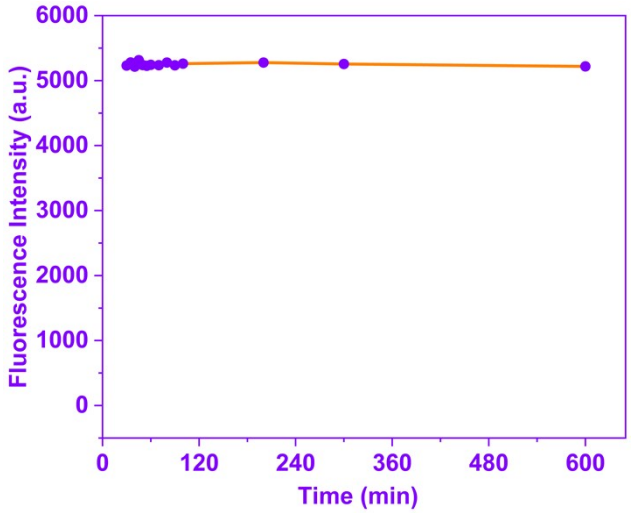

Fig. S15 Fluorescence intensity change of probe ***R1*** (20 μmol·L^{-1}) upon addition of GSH (500 μmol·L^{-1}) under the presence of contentious irradiation by Xe lamp in EtOH–H_2O (1:1, v:v, PBS, pH = 7.4) solution, λ_{ex} = 430 nm.

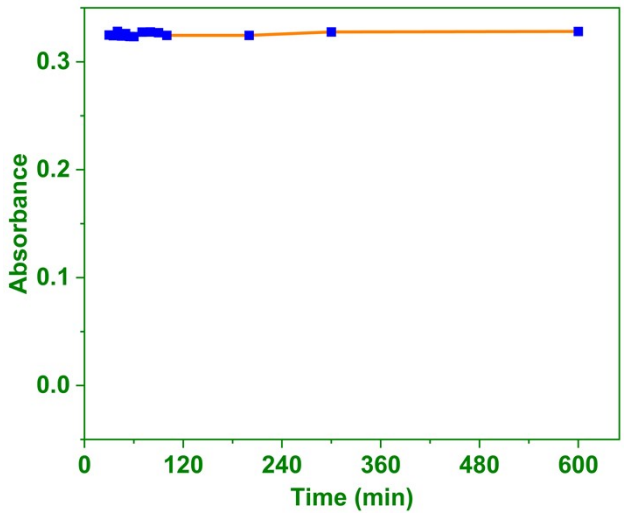

Fig. S16 Absorption intensity change of probe ***R1*** (20 μmol·L^{-1}) upon addition of GSH (500 μmol·L^{-1}) under the presence of contentious irradiation by Xe lamp in EtOH–H_2O (1:1, v:v, PBS, pH = 7.4) solution.

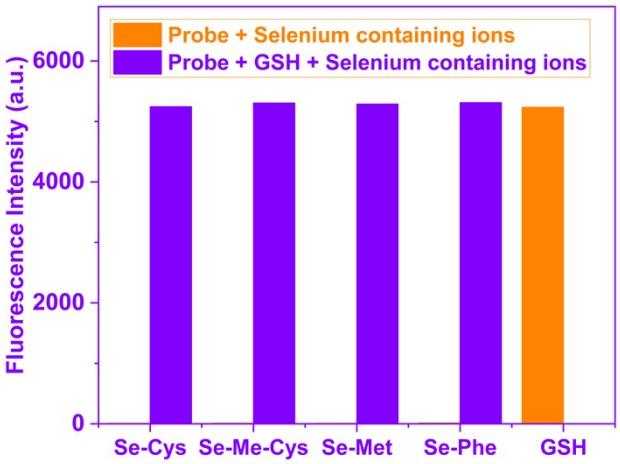

Fig. S17 Selective and Competitive investigation for the fluorescence response of **R1** (20 μmol·L^{-1}) over selenium containing compounds (500 μmol·L^{-1}) in EtOH–H_2O (1:1, v:v, PBS, pH = 7.4) solution, λ_{ex} = 430 nm.

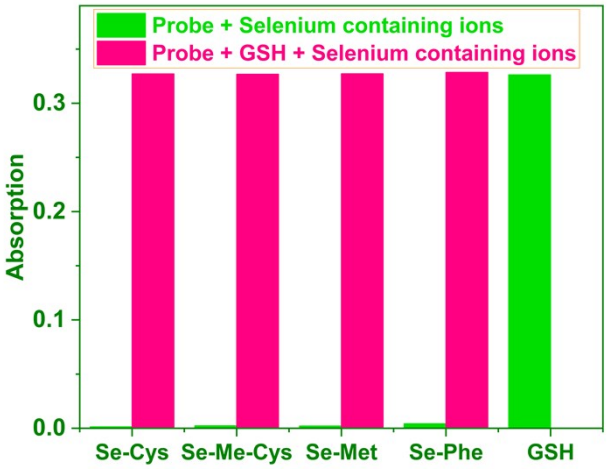

Fig. S18 Selective and Competitive investigation for the absorptionresponse of **R1** (20 μmol·L^{-1}) over selenium containing compounds (500 μmol·L^{-1}) in EtOH–H_2O (1:1, v:v, PBS, pH = 7.4) solution.

2. Calculation of the LOD.

The detection limits were estimated based on the Kaiser's definition:

$y_d = y_b + KS_b$ (off-on)

y_d is the detection limit of the sample. y_b present the mean value fluorescence intensity of the blank samples. S_b is the population standard deviation of the blank. The K value is 3 (M. Belter, A. Sajnog, D. Baralkiewicz, *Talanta*, 2014, **129**, 606.).

Table S1. Fluorescence intensity and the Standard deviation of the blank samples

	Fl. Intensity	Mean value	Standard deviation	$y_d = y_b + KS_b$
Blank #1	5.242	6.211	0.630	8.101
Blank #2	5.873			
Blank #3	6.372			
Blank #4	5.837			
Blank #5	5.362			
Blank #6	6.372			
Blank #7	7.213			
Blank #8	6.432			
Blank #9	6.882			
Blank #10	6.524			

[a] y_d is the detection limit of the sample. y_b present the mean value fluorescence intensity of the blank samples. S_b is the population standard deviation of the blank. The K value is 3.

Table S2. Fluorescence intensity and corresponding concentration of thiols

[GSH] (μmol·L^{-1})	FL. Intensity (GSH)
0.1	6.605
0.2	6.173
0.3	7.615
0.4	8.105
0.5	10.21
0.6	15.11
0.7	21.28
0.8	27.66
0.9	33.07
1	36.21

3. IR, NMR and MS spectra.

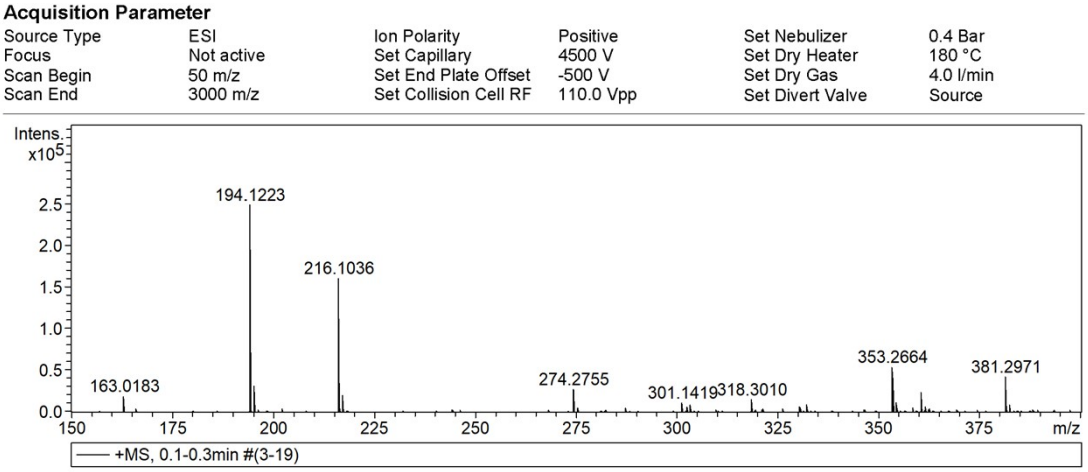

Fig. S19 Mass spectrum of compound **1**.

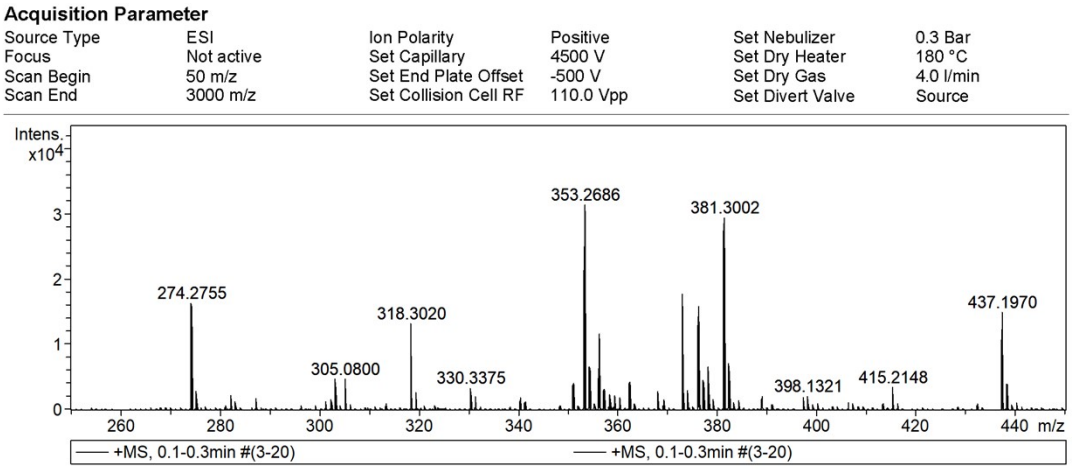

Fig. S20 Mass spectrum of compound **2**.

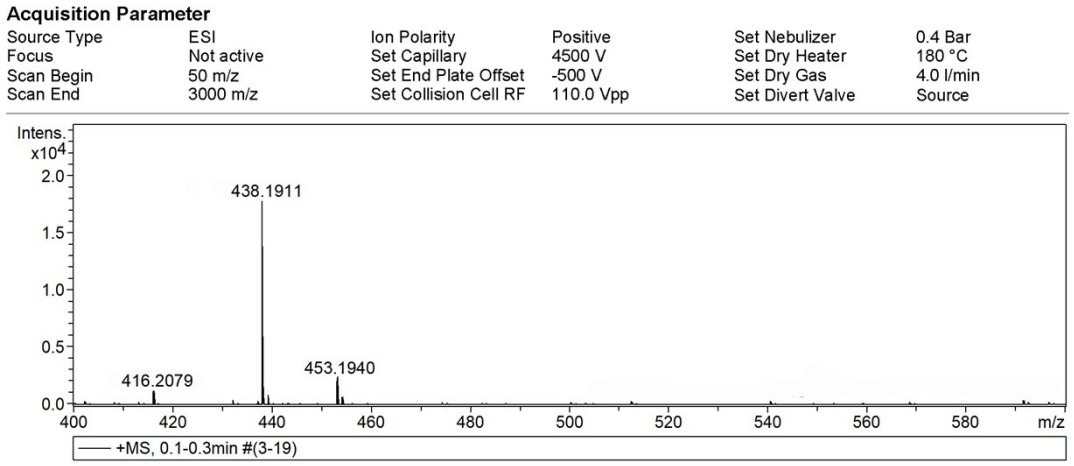

Fig. S21 Mass spectrum of probe ***R1***.

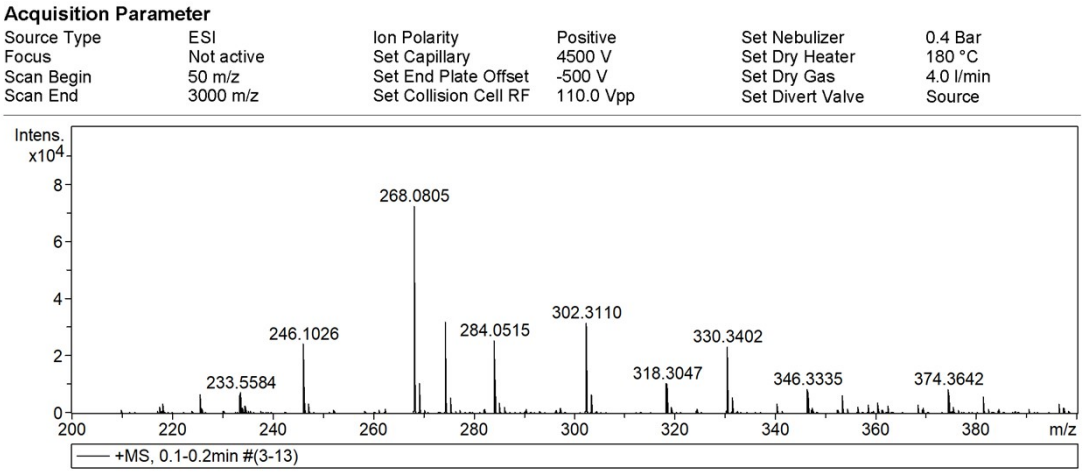

Fig. S22 Mass spectrum of probe ***R1*** + GSH.

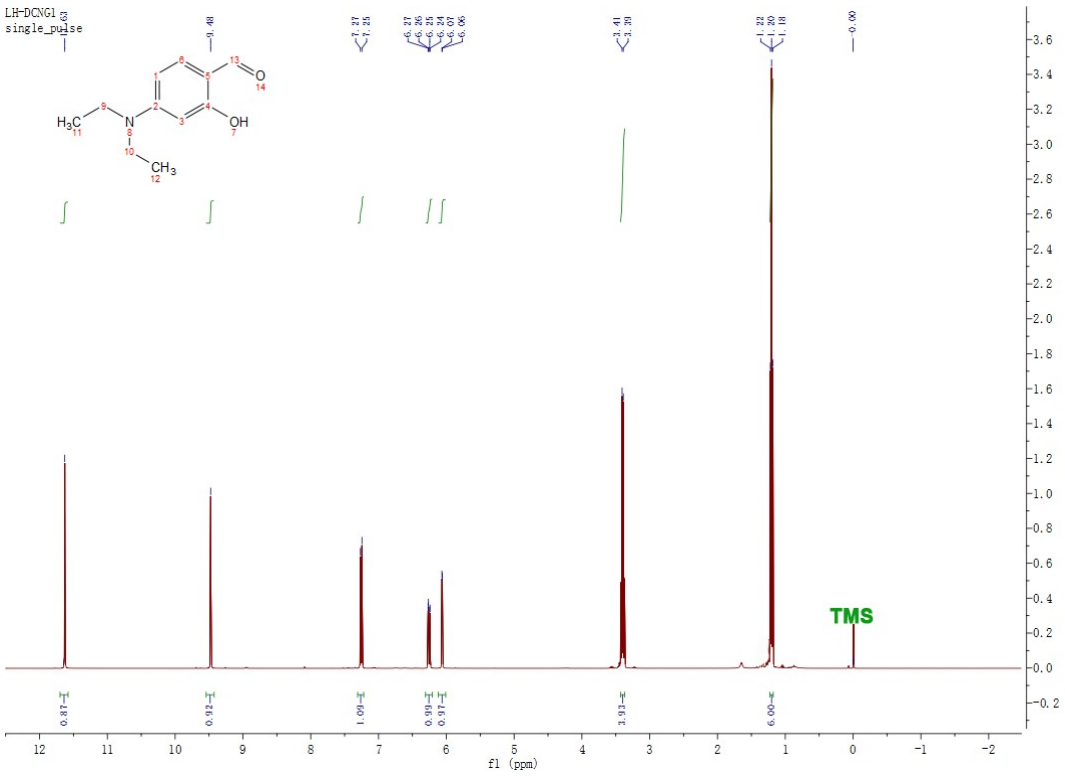

Fig. S23 ^{1}H NMR spectrum of compound **1** in $CDCl_3$.

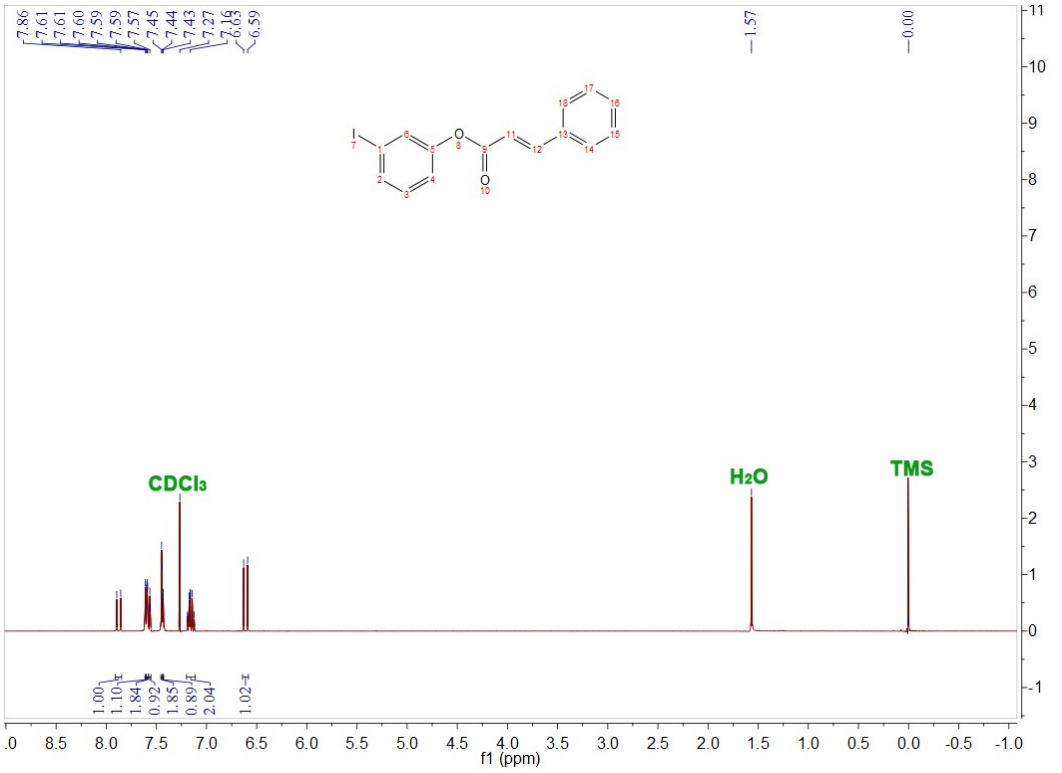

Fig. S24 ^{1}H NMR spectrum of compound **2** in $CDCl_3$.

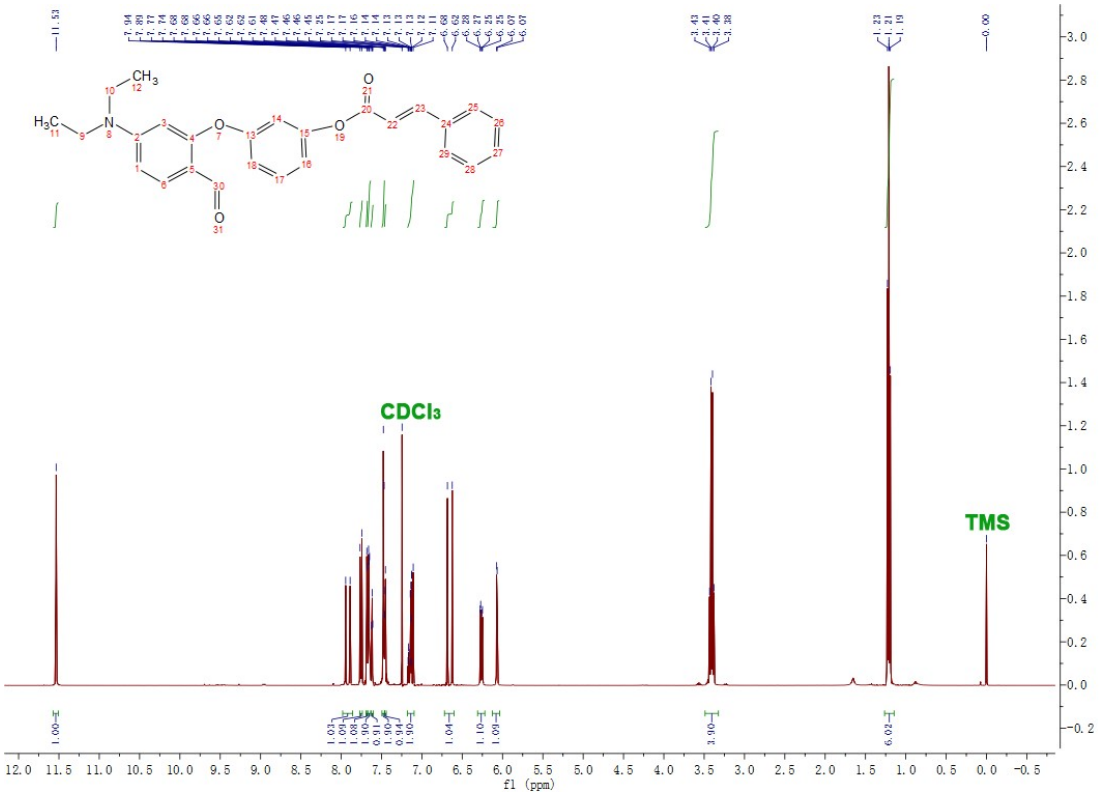

Fig. S25 ^{1}H NMR spectrum of probe ***R1*** in $CDCl_3$.

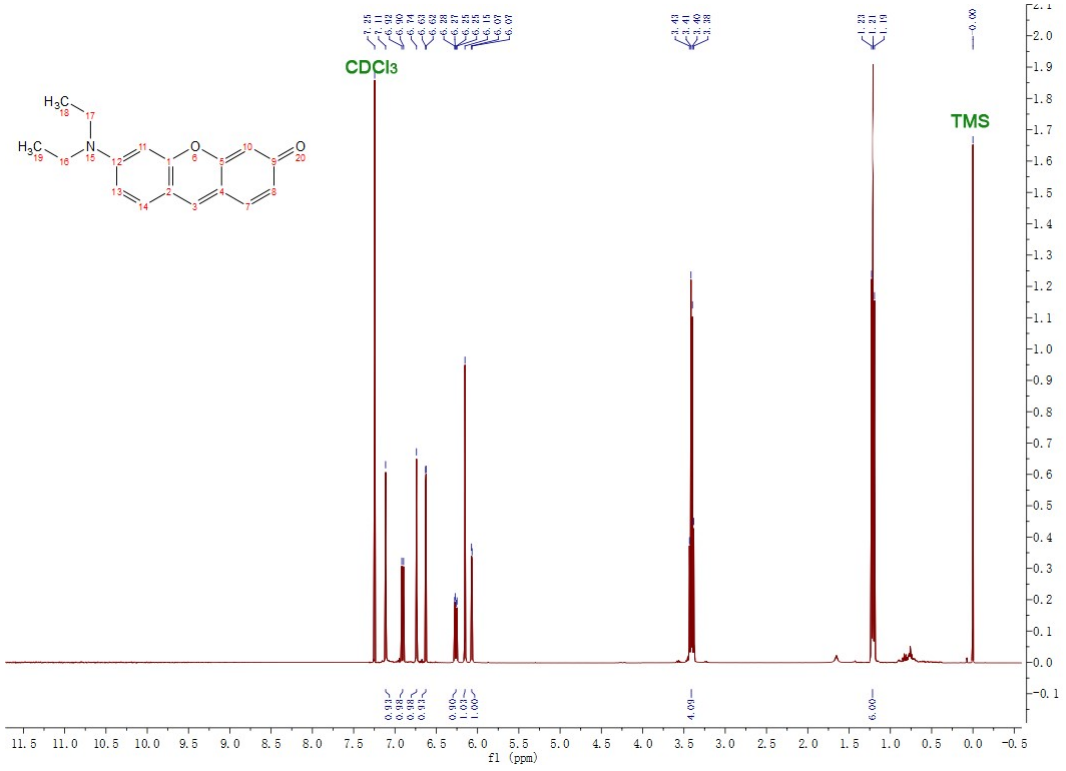

Fig. S26 ^{1}H NMR spectrum of probe ***R1*** + GSH in $CDCl_3$.

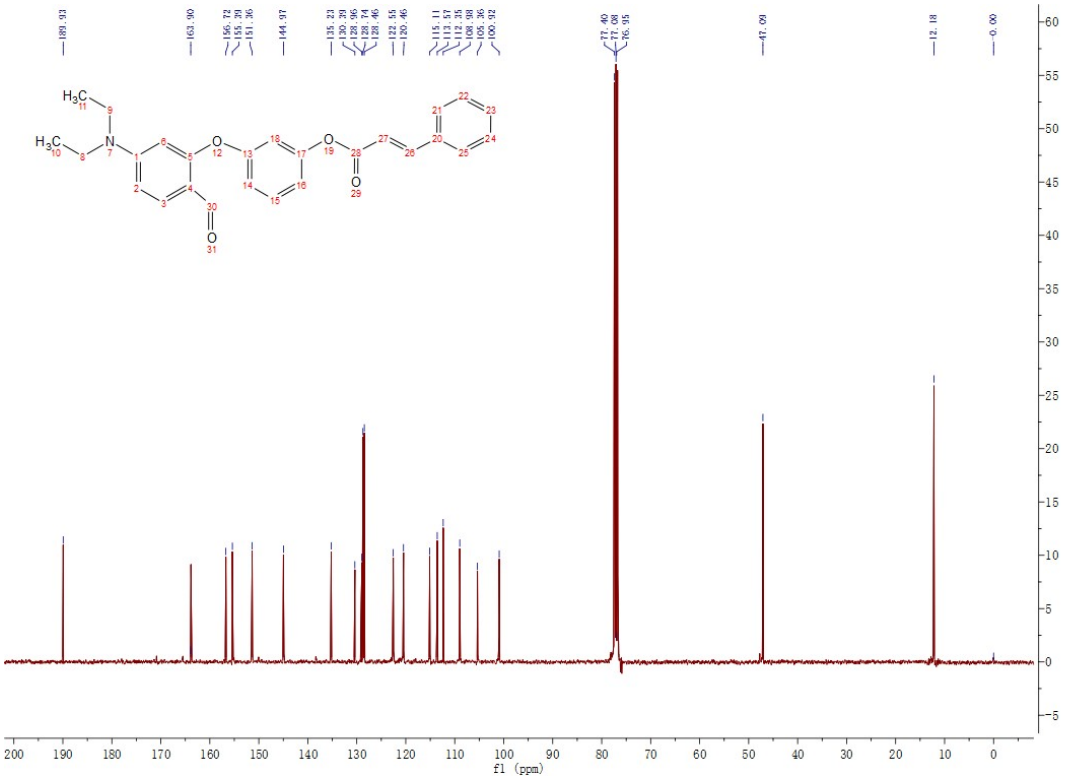

Fig. S27 ^{13}C NMR spectrum of probe ***R1*** in $CDCl_3$.

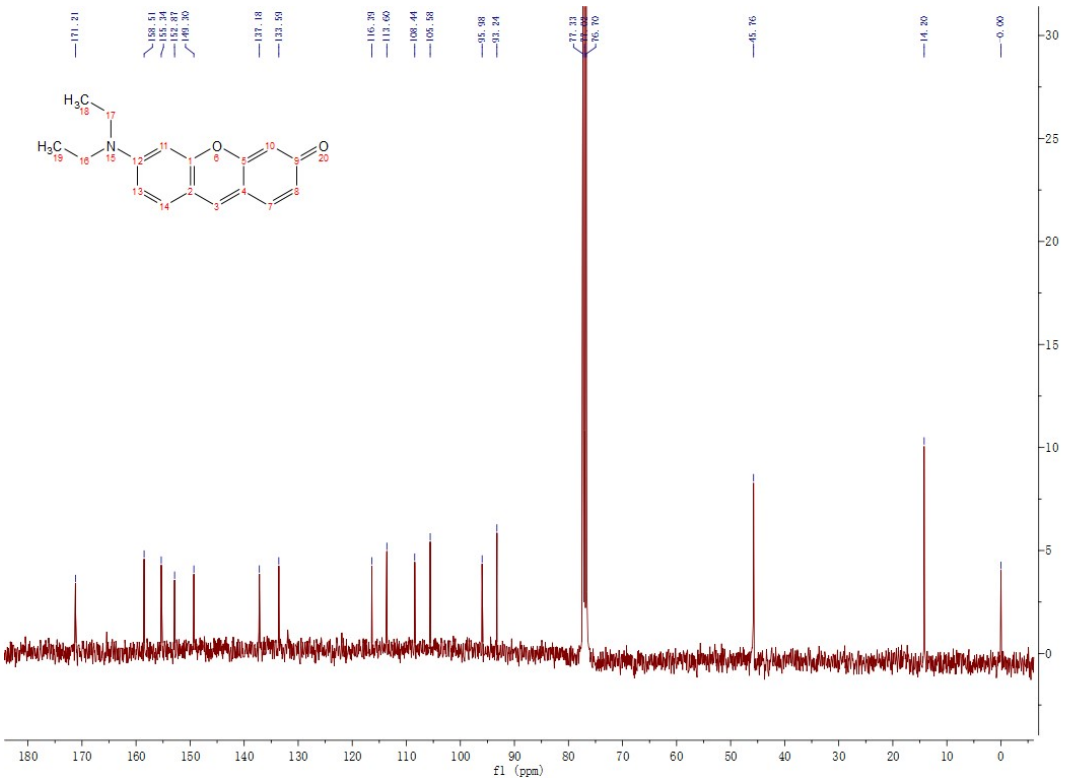

Fig. S28 ^{13}C NMR spectrum of probe ***R1*** + GSH in $CDCl_3$.

4. Theoretical calculation

All theoretical calculations including HOMO/LUMO energies and electrostatic potential (ESP) were performed by the Gaussian 09 program. The geometry optimization of ground states was computed with density functional theory (DFT). The probe was optimized with a combination of basis of double-ζ quality consisting of 6-31G** for C, H elements, 6-31+G* for N, O elements. All the optimized structures were confirmed to be local minimums due to the non-existence of imaginary frequency.

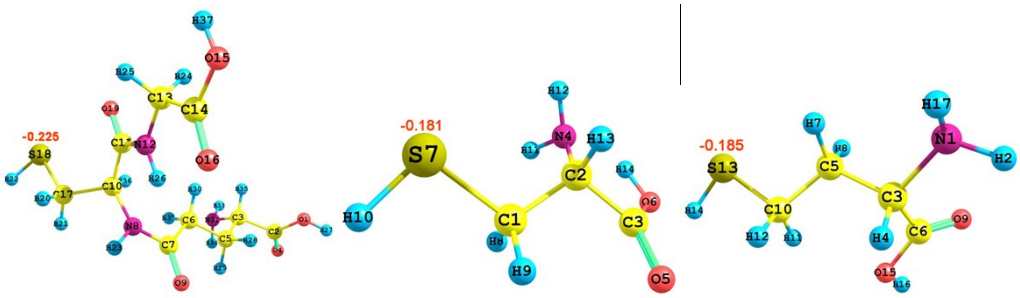

Fig. S29 The optimized structures and electrostatic potentials of GSH, Cys and Hcy.

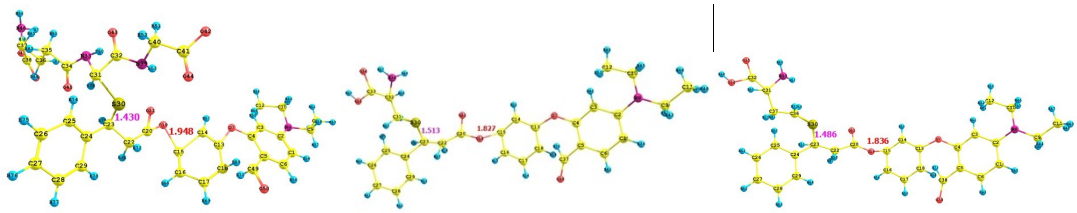

Fig. S30 The optimized structures and bond lengths of probe R1 with addition of GSH, Cys and Hcy.

Table. S3 Electrostatic potential of sulfur atom in three thiols and BDE of C-O bond in three transition-state molecules.

Name	Electrostatic Potential[a]	Name	BDE (KJ·mol^{-1})[b]
GSH	-0.079	**R1**+GSH	35.2312
Hcy	-0.044	**R1**+Hcy	52.3287
Cys	-0.059	**R1**+Cys	55.3276

[a] Electrostatic potential of sulfur atom in three thiols.

[b] Bond dissociation energy.

5. MTT assay results of the probe.

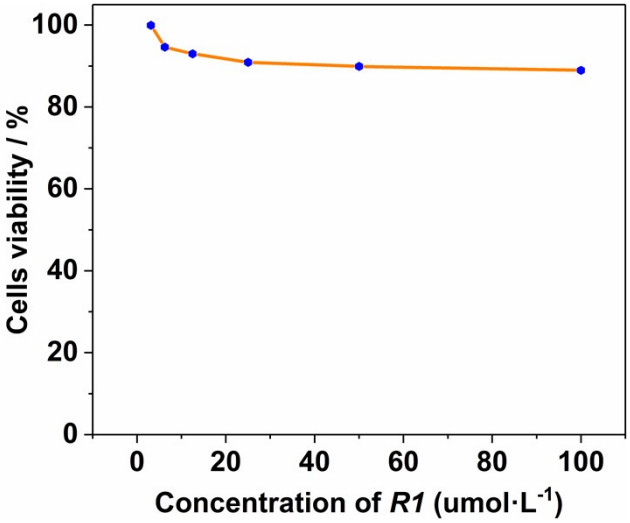

Fig. S31. The influence of cell viability with the change of ***R1*** concentration.

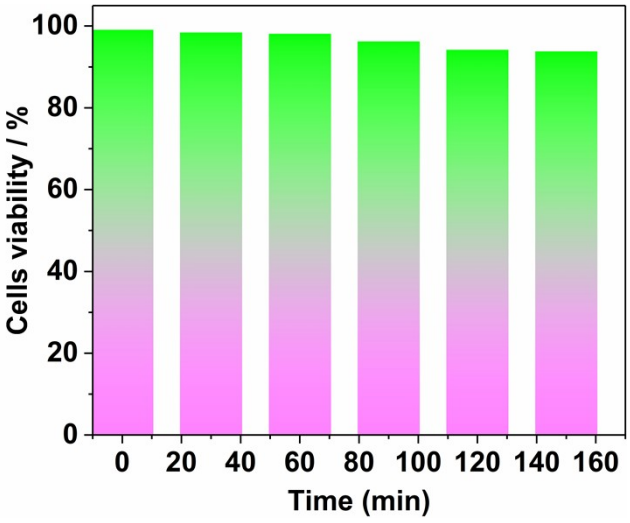

Fig. S32. The relationship between cell viability and incubation time.

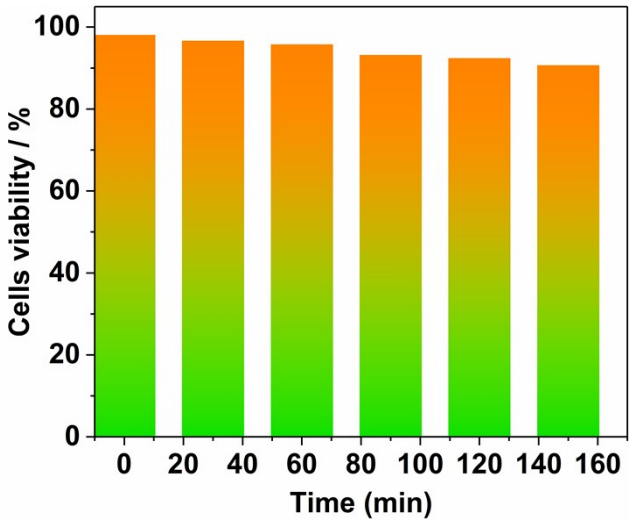

Fig. S33. The relationship between cell viability and incubation time in addition of 20 μmol·L^{-1} of ***R1***.

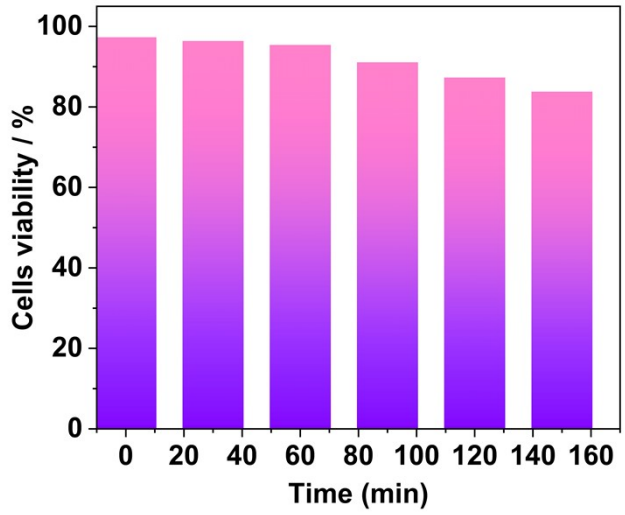

Fig. S34. The relationship between cell viability and incubation time in addition of 20 μmol·L^{-1} of ***R1*** and 25 equiv. of GSH.

Table S4. MTT assay results, calculated inhibition ratio and IC_{50} value of the probe ***R1*** for MG-63 cell.

[***R1***]/μM	1	2	3	Average	Inhibition ratio	IC_{50}/μM
3.125	0.458	0.471	0.465	0.4647	0.0005	>100
6.25	0.435	0.432	0.453	0.4400	0.0536	
12.5	0.432	0.421	0.444	0.4323	0.0701	
25	0.423	0.413	0.432	0.4227	0.0909	
50	0.411	0.422	0.421	0.4180	0.1009	
100	0.402	0.427	0.412	0.4137	0.1102	